

Separate CT-Reconstruction for Orientation and Position Adaptive Wavelet Denoising

Anja Borsdorf^{1,2}, Rainer Raupach², Joachim Hornegger¹

¹Chair for Pattern Recognition, Friedrich-Alexander-University Erlangen-Nuremberg

²Siemens Medical Solutions, Forchheim

Email: anja.borsdorf@informatik.uni-erlangen.de

Abstract. The projection data measured in computed tomography (CT) and, consequently, the slices reconstructed from these data are noisy. For a reliable diagnosis and subsequent image processing, like segmentation, the ratio between relevant tissue contrasts and the noise amplitude must be sufficiently large. By separate reconstruction from even and odd numbered projections, two images can be computed, which only differ with respect to noise. We show that these images allow an orientation and position adaptive noise estimation for level-dependent threshold determination in the wavelet domain.

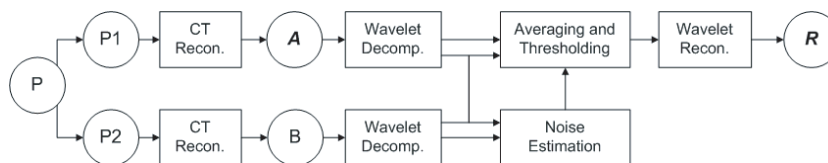
1 Introduction

In computed tomography (CT), the projections acquired at the detector are noisy, predominantly caused by quantum statistics. This noise propagates through the reconstruction algorithm to the reconstructed slices. Pixel noise in the images can be reduced by increasing the radiation dose or by choosing a smoothing reconstruction [1]. However, with respect to patient care, the least possible radiation dose is required and a smoothing reconstruction lowers image resolution. This shows that pixel noise in the images cannot be reduced arbitrarily.

Nevertheless, an increased signal-to-noise ratio is beneficial for a reliable diagnosis and subsequent image processing, like registration or segmentation. This paper presents a new wavelet based method for edge-preserving noise reduction in CT-images.

2 State of the art and new contribution

A very important requirement for any noise reduction in medical images is that all clinically relevant image content must be preserved. A common approach for edge-preserving noise reduction is wavelet thresholding, based on the work of Donoho and Johnstone [2]. The input image is decomposed into wavelet coefficients. Insignificant detail coefficients below a defined threshold are erased, but those with larger values are preserved. The noise suppressed image is obtained

Fig. 1. Block diagram of the noise reduction method

by an inverse wavelet transformation from the modified coefficients. The difficulty is to find a suitable threshold, especially for noise with spatially varying power and directed noise, which is commonly present in CT-images. Choosing the threshold too high may lead to visible loss of image structures, but the effect of noise suppression may be insufficient, if the threshold was chosen too low. Therefore, a reliable estimation of noise for threshold determination is one of the main issues.

We show that the local and orientation dependent noise power in CT can be estimated from two separately reconstructed images, which only differ with respect to image noise. Therefore, the noise reduction method adapts itself to the noise power and allows for the reduction of spatially varying and oriented noise.

3 Methods

3.1 Overview

An overview of the noise reduction method is shown in Fig. 1. First, two images A and B are generated, which only differ with respect to image noise. In CT, this can be achieved by separate reconstruction from disjoint subsets of projections $P1 \subset P$ and $P2 \subset P$, with $P1 \cap P2 = \emptyset$. More precisely, one image is reconstructed from the even and the other from the odd numbered projections. The two resulting images include the same information but different noise. Both images are decomposed by a two dimensional stationary wavelet transformation (SWT) [3]. After this transformation, at each decomposition level, four two-dimensional blocks of coefficients are available for both images: the lowpass filtered approximation image C and three detail images W^H , W^V and W^D including high frequency structures in horizontal (H), vertical (V) and diagonal (D) direction, together with noise in the respective frequency bands. The computation of the differences between the detail coefficients of the two input images shows just the noise in the respective frequency band and orientation. These noise images can then be used for the estimation of the spatial and orientation dependent standard deviation of noise in A and B . From this estimation, a thresholding mask is computed and applied to the averaged detail coefficients of the input images. The computation of the inverse wavelet transformation from the modified coefficients results in a noise-suppressed image. This again corresponds to the reconstruction from the complete set of projections but with improved signal-to-noise ratio.

3.2 Threshold determination

The two images A and B only differ with respect to image noise, but include the same information

$$A = S + N_A, \quad B = S + N_B \quad (1)$$

where S represents information and $N_A \neq N_B$ noise included in image A and B , respectively. The standard deviations of noise in the two separately reconstructed images can be assumed to be equivalent ($\sigma_A \approx \sigma_B$), because the number of contributing quanta for both images is approximately the same. However, the noise level in A and B is increased by a factor of $\sqrt{2}$ in comparison to the reconstruction from the complete set of projections or the average of the two input images $M = 0.5(A + B)$. It can be assumed that we have zero-mean noise in both images. By the computation of the difference image

$$D = A - B = N_A - N_B \quad (2)$$

we get a noise-image free of structures. The standard deviations σ_A and σ_B of noise can be approximated from the standard deviation in the difference image σ_D by

$$\sigma_A = \sigma_B = \frac{\sigma_D}{\sqrt{2}} \quad (3)$$

Thus, the standard deviation of noise in the average image M results in:

$$\sigma_M = \frac{\sigma_A}{\sqrt{2}} = \frac{\sigma_D}{2} \quad (4)$$

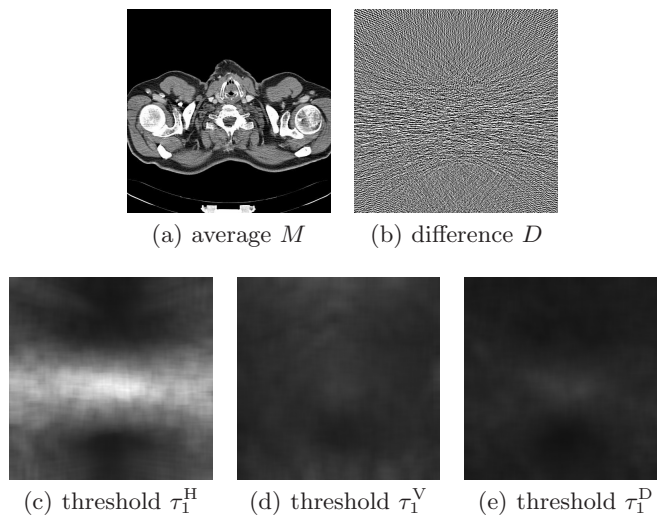
In order to compute a level and orientation dependent threshold for denoising in the wavelet domain, noise in the different frequency bands and orientations should be estimated in separation. The discrete wavelet transformation is a linear transformation. Therefore, the differences between the detail coefficients can also be directly used for noise estimation. At each decomposition level l the difference images

$$D_l^H = W_{Al}^H - W_{Bl}^H, \quad D_l^V = W_{Al}^V - W_{Bl}^V, \quad D_l^D = W_{Al}^D - W_{Bl}^D \quad (5)$$

between the detail coefficients are computed, where the subscripts A and B correspond to the two images. These difference images are then used for the estimation of noise in the respective frequency band and orientation. In CT-images, the noise power is spatially varying. Therefore, noise should be estimated position dependent. In order to achieve this, a region of $m \times m$ pixels is chosen around each position in the difference image and the standard deviations of the pixel values are locally computed within these regions. Thus, we obtain three images σ_l^H , σ_l^V and σ_l^D with the local standard deviations of noise in the difference images in the horizontal, vertical and diagonal directions. Together with Eq. (4), orientation, position and level dependent thresholds are computed

$$\tau_l^H = k \frac{\sigma_l^H}{2}, \quad \tau_l^V = k \frac{\sigma_l^V}{2}, \quad \tau_l^D = k \frac{\sigma_l^D}{2} \quad (6)$$

Fig. 2. Example of orientation and position dependent threshold at the first decomposition level for thoracic image with strongly directed noise



The constant k controls the amount of noise suppression. With increasing k more noise is removed. In Fig. 3(c)- 3(e) the thresholds computed with $m = 32$ for the first decomposition level in the horizontal, vertical and diagonal directions are shown for a thorax-slice (see average of input images in Fig. 3(a)) with strongly directed noise (see difference of input images in Fig. 3(b)).

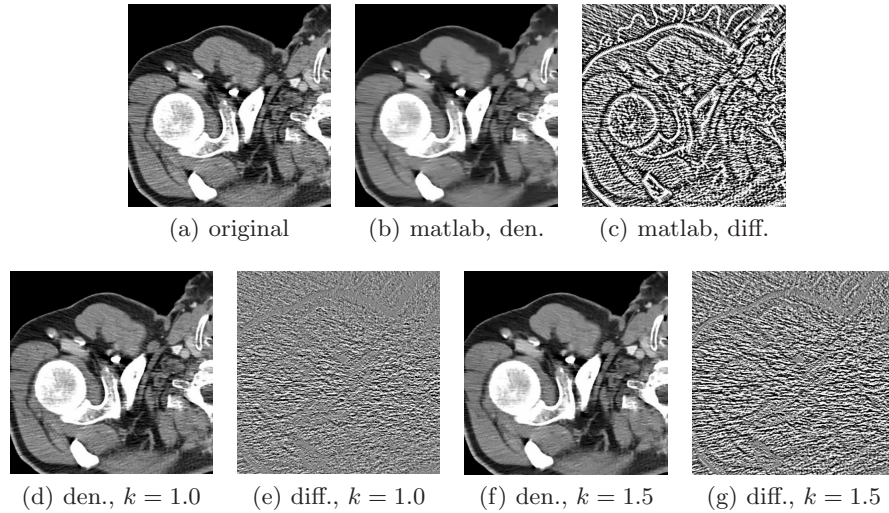
3.3 Averaging and thresholding

The computed thresholds from Eq. (6) are then applied to the averaged wavelet coefficients of the input images. We perform a *hard* thresholding, meaning that all coefficients with an absolute value below the threshold are set to zero and values above are kept unchanged. The final noise suppressed image is computed by an inverse wavelet transformation from the averaged and weighted wavelet coefficients of the input images.

4 Results

In Fig. 4(d) and 4(f), zoomed-in noise suppressed results from the proposed method applied to a thoracic image (see Fig. 3(a)) are shown for two different settings of k . Further, the difference images (Fig. 4(e), 4(g)) between the denoised and average of input images (Fig. 4(a)) are displayed. The images are compared to the denoising result achieved with the *SWT De-noising 2D* tool from the Matlab wavelet toolbox [4] (see Fig. 4(b) and 4(c)). All computations were performed using a Haar wavelet decomposition up to the fourth decomposition level. For denoising in Matlab, we used a *Balance Sparsity-Norm* hard thresholding method with a non-white-noise model.

Fig. 3. Denoising result of the proposed method in pixel region taken from thorax-slice with strongly directed noise. Center and window settings used for displaying CT-images: $c = 50$, $w = 400$. Center and window settings used for displaying difference images: $c = 0$, $w = 30$



5 Discussion

The difference image in Fig. 4(c) shows that standard wavelet denoising methods reduce noise in the images but also blurr edges. The reason for this is that no reliable noise estimation is possible if just one CT-image is available. In contrast, the proposed method adapts itself to the spatially varying noise power in the different frequency bands and orientations and, therefore, performs much better especially in images with directed noise.

References

1. Kalender WA. Computed Tomography. Munich: Publics MCD Werbeagentur GmbH; 2000.
2. Donoho DL, Johnstone IM. Ideal spatial adaptation by wavelet shrinkage. *Biometrika* 1994;81(3):425–455.
3. Coifman RR, Donoho DL. Translation invariant denoising. *Lecture Notes in Statistics: Wavelets and Statistics* 1995;103:125–150.
4. Mathworks Inc. Wavelet Toolbox; 2006. <http://www.mathworks.com/products/wavelet/>.